APPLICATION OF A CAUSAL DIGRAPH BASED FAULT DIAGNOSIS METHOD WITH DISCRETE STATE SPACE MODEL ON A PAPER MACHINE SIMULATOR

Hui Cheng, Mats Nikus, Sirkka-Liisa Jämsä-Jounela

Helsinki University of Technology
Laboratory of Process Control and Automation
Kemistintie 1, FI-02150 HUT, Finland

Abstract: The aim of the work presented in this paper is to evaluate the ability of the causal digraph method to detect and isolate faults on a simulated paper machine process. In order to represent the causal relations between the variables using discrete state space models, a linearity test was performed for the short circulation sub process in the papermaking simulator. The corresponding causal digraph model was constructed, identified and used to detect and locate the artificial fault in the simulation environment. The studied fault was a drop in the fiber acceptance rate of the pressure screen before the deculator.

Keywords: Fault detection, Fault isolation, causal digraph, papermaking, APROS simulator, CUSUM, short circulation

1. INTRODUCTION

Due to the increasing competition in the process industries, there has been a strong need to detect, locate and estimate faulty states and recover the process from these states. By applying fault diagnosis, process safety, product quality and equipment maintenance could be improved remarkably.

Since Iri et al. (1979) introduced the Signed Directed Graph (SDG), the simplest causal digraph method, into the field of process fault diagnosis, it has made remarkable progress and been the most popular causal model based method for process fault diagnosis. In order to alleviate the problem with spurious results, fuzzy logic was used by Shih and Lee (1995a, 1995b) to represent both the variables and the relations in the causal digraph. However the method itself still remained static. Another big improvement of the causal digraph was the introduction of the piece-wise linear transfer functions (QTF) by Leyval et al. (1994). The used simplified transfer function provides dynamic information. With the introduction of the QTF a new reasoning method for diagnosis purposes was based on residuals was needed. Recently more quantitative models, such as difference-algebraic equations (Montmain and Gentail, 2000) have been used in causal digraph to further improve the diagnosis results.

The aim of this paper is to evaluate the fault detection and isolation abilities of the causal digraph method on paper machines. In this study, the APROS simulator developed by VTT (Technical research center of Finland) was used to simulate the papermaking process (APROS, 2005) and NNDT (Saxén B. and H. Saxén, 1994) was used to identify the discrete state space model in the causal digraph model. In this paper the causal relations are represented by state space models. The fault detection and isolation steps were performed using the developed MATLAB graphic user interface.

The paper is organized as follows. In the next section the basic concepts about FDI, causal digraphs and the CUSUM method will be described. Section 3 describes the short circulation process in paper mills and the studied fiber acceptance rate drop fault. In section 4, the linearity of the APROS paper machine model was proved and the causal digraph model is constructed using the MATLAB user interface. The fault diagnosis results are shown in section 5 followed by the conclusions in section 6.

2. FAULT DETECTION AND ISOLATION (FDI)

In both process industries and the academic world, a fault is usually considered as an undesired deviation of the system structure and parameters from their nominal state. Fault detection and isolation refer to detecting the occurrence of a fault in a process and locating the faulty components respectively. Due to active research during the last two decades, dozens of new FDI methods have been developed. However, most of the methods are carried out using a similar procedure entailing residual generation, residual evaluation and decision-making. In this paper, the residuals are generated using a causal digraph model and evaluated with the CUSUM method. The final decision is made according to the causal digraph reasoning rules.

2.1 Causal digraphs

Causal graphs provide a good way to represent physical cause-effect relations between different process variables that are of interest for fault diagnosis. In the causal directed graph models, the nodes denote the variables, while the directed edges between the nodes represent the causal relations between these variables, through which faults can propagate.

Different models can be used to explain the cause-effect relations on the edges depending on the nature and level of abstraction of the model, which subsequently leads to a variety of different methods for backward (diagnosis) and forward (simulation) reasoning. The Signed Directed Graph (SDG) method, the simplest causal directed graph method, uses pure qualitative information, which can give rise to ambiguous fault diagnosis. The more recent use of QTF and difference equations has introduced more quantitative information into the model and consequently decreased the amount of spurious results.

2.2 Residual generation

Causal digraphs produce two kinds of residuals to be used in fault detection and isolation. The global residuals (GR) are obtained as the difference between the measurement and the global propagation value shown below:

$$\delta(k) = y(k) - \hat{y}(k) \tag{1}$$

where *y(k)* is the measurement and $\hat{y}(k)$ is the global propagation value obtained by

$$\hat{y}(k) = f(\hat{U}(k-1), \hat{U}(k-2),..) \tag{2}$$

where in dynamic cases $\hat{U}(k-1) = [\hat{u}_1(k-1),....\hat{u}_n(k-1)]^T$ is the lagged global propagation values from the parent nodes in the graph model and *n* denotes the number of the inputs for the variable *y*.

The local residual can be further subcategorized into three types: individual local residual (ILR), multiple local residual (MLR) and total local residual (TLR).

The individual local residual can be produced by taking the difference between the measurement and the local propagation value with only one measured input while all the others are propagation value from parent nodes.

$$ILR(m) = y(k) - f(U_m(k-1), U_m(k-2),...) \tag{3}$$

where $U_m(k-1) = [\hat{u}_1(k-1),..u_m(k-1),..\hat{u}_n(k-1)]^T$, the $\hat{u}_i(k-1)$ is the global propagate value from the parent node, and the $u_j(k-1)$ is the measurement for the parent nodes. Usually the number of ILRs is the same as the number of inputs to the model for predicting the variable *y*.

Similarly the MLR is produced by

$$MLR(m,d) = y(k) - f(U_{m,d}(k-1), U_{m,d}(k-2),...) \tag{4}$$

where

$U_{m,d}(k-1) = [\hat{u}_1(k-1),..u_m(k-1),.u_d(k-1),..\hat{u}_n(k-1)]^T$

and *m, d* denote the inputs for variable *y* with measurement value. Generally the MLRs can be produced for all possible combinations inputs to the model for variable *y*.

The TLR is produced by

$$TLR = y(k) - f(U(k-1), U(k-2),...) \tag{5}$$

where $U(k-1) = [u_1(k-1),..u_n(k-1)]^T$ is the lagged measurement values for all inputs to the model for variable *y*.

2.3 Residual evaluation

The nature of the residual evaluation in this method is a mapping from the residuals to the set {0,1}. In the faultless case, the residuals are considered to be a zero mean random sequence signal, for which the mean value will change when a fault occurs.

For the detection of a jump in the mean of a noisy residual, the CUSUM method by Page and Hinckley was implemented. For a positive mean jump, the following applies.

$$SUM(k) = SUM(k-1) + \delta(k) - \mu_0 - minfault/2 \tag{6}$$

$$MinSUM = \min_{n<k} SUM(n) \tag{7}$$

where *minfault* is a user specified minimum detectable jump. When $SUM(k) - MinSUM > \lambda$, a jump has been detected (Hinckley, D. V., 1971). The parameter λ provides some robustness to the fault detection but it will also delay the detection. A more general procedure can be developed based on the simple positive jump case for detecting two-directional jumps and residual recovery back to the normal situation.

minfault and λ are design parameters, usually tuned according to the requirement for false alarm and missed alarm rates. Theoretically the CUSUM method can detect very small jumps in the mean, but in practice, *minfault* is decided by the minimum detectable fault and λ is usually set to 10-20 times of *minfault.*

With the CUSUM method, the generated residuals above are mapped into 0 or 1, which can be used in the fault diagnosis reasoning with the rules presented in the following section.

2.4 Fault diagnosis reasoning

With the results obtained from the residual evaluation, the structural information in the causal digraphs can be used to diagnose faults. There are two types of rules concerning fault diagnosis: fault location rules and fault nature rules.

For a specific node *y* in the causal digraph, the fault location rules can locate the fault on the variables even in the presence of multiple alarm variables. The reasoning rules for faults location are shown in the Table 1.

Table 1 Causal digraph fault location rules

GR	TLR	ILR(m)	MLR(m,d)	Location
0	0	0	0	No fault
1	0	1	0	Upstream
1	0	0	0	Upstream
1	1	1	1	Local

After the locating the fault origin, in most cases the nature of the fault can be identified by fault nature rules, which are given in the following table.

Table 2 Causal digraph fault nature rules

GR for any child node	TLR for any child node	Fault nature
1	1	Local fault for that child node
1	0	Parameter fault
0	1	Sensor fault

3. CASE STUDY

This paper provides a case study concerning fault detection and isolation on a paper machine simulator. The focus is on the short circulation process but paper quality variables are considered as well. For this study, the Advanced Process Simulator (APROS) was used to build the paper machine model. For a general description of the APROS simulator, the reader is referred to the APROS website (APROS, 2005). In the remainder of this section, the short circulation process is described together with a presentation of the studied fault.

3.1 Short circulation process

The short circulation is a crucial part of the papermaking process, with several important functions. The dilution of the fiber-suspension entering the process to a suitable consistency for the headbox takes place in the short circulation, in a mixing process were low-consistency water from the wire-pit is mixed with high-consistency stock. The second important task of the short circulation is the removal of impurities and air. This task is performed in the hydro-cyclones, machine screens and the so-called deculator. The short circulation also improves the economy of the process because the valuable fibres and filler materials that pass through the wire are recycled. As the intermediate process between stock preparation and former, the short circulation process is very important for paper quality control, since the basic weight, ash consistency and stock jet ratio control are performed in the short circulation part.

The short circulation process starts after a machine chest. Usually the machine chest is followed by a thick stock pump and a basic weight valve, which is used for basic weight control. The thick stock is pumped to the wire pit and mixed with white water and filler controlled by the filler valve. The diluted stock is pumped by a fan pump via the hydro-cyclones to the deculator. The deculator has a continuous overflow to keep the inlet pressure constant for the head box feed pump. The diluted stock is then pumped into the hydraulic headbox and sprayed onto the wire at a constant speed. On the wire the stock is dehydrated to form a wet web. About 98% of the water and 54% of the filler and fibre go through the wire and flow to the wire pit as white water. The process is presented in Figure 1.

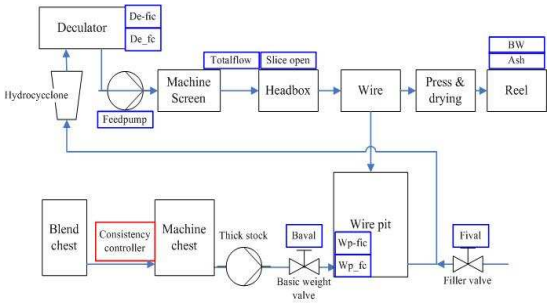

Fig. 1. Flow sheet of the short circulation process.

The variables shown in Figure 1 are important for building the causal digraph model. Table 3 gives a description of the variables.

Table 3 Description of the variables in the short circulation

Variables	**Description**	**Unit**
baval	Basis weight valve opening	-
wp_fc	Filler consistency in the wire pit	%
wp_fic	Fiber consistency in the wire pit	%
fival	Filler adding valve opening	-
de_fc	Filler consistency in the deculator	%
de_fic	Fiber consistency in the deculator	%
feedpump	Headbox feed pump rotation	%
totalflow	Mass flow into the headbox	kg/s
bw	Basis weight of paper	g/m^2
ash	Ash consistency of paper	%

The APROS simulator provides first principle models for the necessary components, with which the model for the paper machine was constructed and parameterized. Figure 2 shows the model used for this case study.

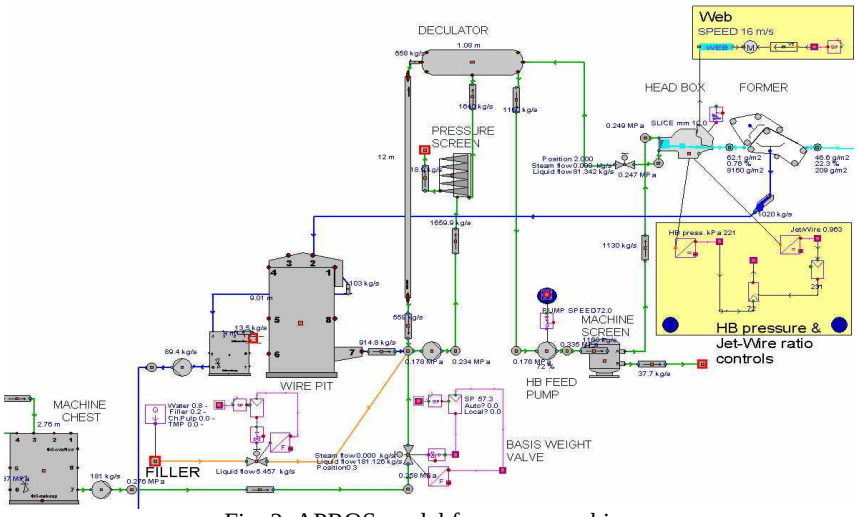

Fig. 2. APROS model for paper machine

3.2 Faulty case

As a serious fault in the paper making industry, drops in the pressure screen fiber acceptance rate can cause problems even though the quality control loop could compensate the fault effect on the final product quality. A low acceptance rate arising from the malfunction of pressure screen will make it difficult to transfer fibers from the machine chest section to the deculator decreasing the efficiency significantly. The corresponding artificial fault was simulated in the APROS model were the fiber acceptance rate in pressure screen dropped from the nominal value 95% to 94%. In the faulty case, the value of fiber consistency in deculator, headbox and wire pit will all increase over the thresholds and cause alarm. The need to find the fault origin as well as the nature of the fault in these situations is well met by causal digraphs.

4. MODEL CONSTRUCTION

4.1 Linearity test

In this paper dynamic models were used to describe the relations between the variables of equation 2. Before the dynamic modeling the linearity of the APROS paper machine model was tested, since the detailed mathematic model for it was unknown.

Among all the variables in Table 3, *baval*, *fival* and *feedpump* are actuator input signals corresponding the input nodes in the causal digraph. By opening the control loop for the paper machine and manipulating the actuator signal manually, the data of 64 different steady states was collected from the simulator. From the knowledge of the process and the collected data, the structure of the causal digraph can be defined and shown as in figure 3.

The linearity between related variables is tested in two ways. For those variables that have only one input in the digraph in figure 3, the steady points (input vs. output) was plotted and tested. One example is given in figure 4 for the fiber consistency in the headbox.

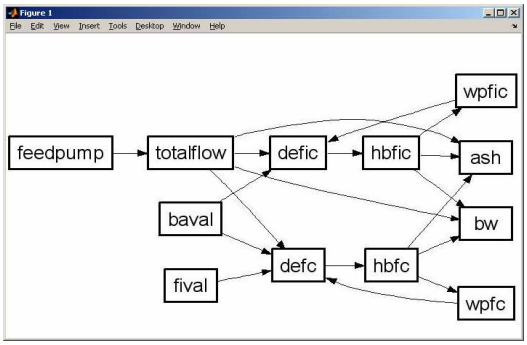

Fig.3. Causal digraph model

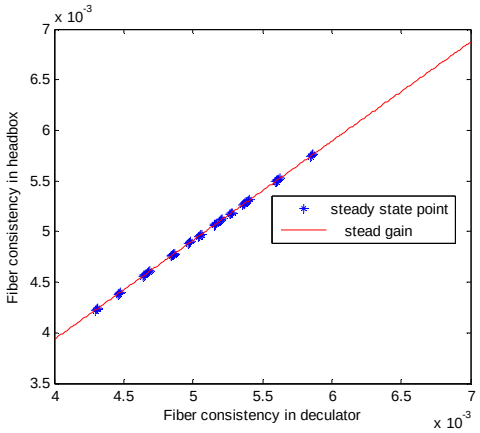

Fig.4. Linearity test for fiber consistency in the headbox

Another way to test linearity is to build a steady state static model for the tested variable with 32 steady states data using the least square method, and test the model with the remaining 32 steady states. One example is shown in figure 5 for the basis weight variable.

The test result shows that the APROS paper machine model is relatively linear, which gives us a reason to use linear state space models when representing causal relations according to equation 2.

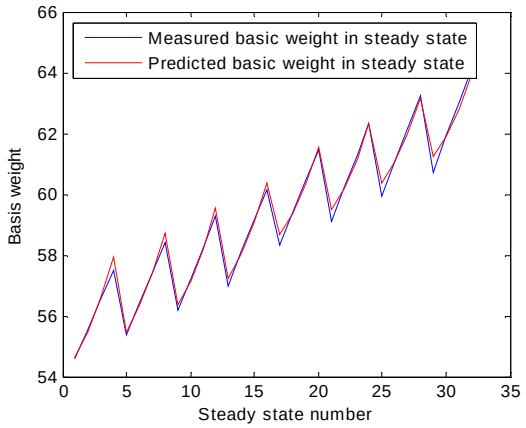

Fig.5. Linearity test for basis weight

4.2 MATLAB graphic user interface

The inputs and outputs variables for state space models were selected according to the structure of digraph in figure 3. New training data and validation data for state space model identification were collected from the APROS simulator under fault free and open loop conditions. The data was then imported to the NNDT software package, which besides neural network training also supports identification of linear structures such as discrete state-space models (Nikus and Bulsari, 1995).

In order to apply the causal digraph method for fault diagnosis more easily, a MATLAB graphical user interface was developed to have such functionalities as: specify the graph, generate the residuals (GR, ILR, MLR, TLR), detect the change with CUSUM and diagnose the fault according to the reasoning rules.

In the interface, nodes and connections between nodes can be specified for the digraph structure. A from the specifications automatically generated digraph is shown in figure 3.

5. RESULTS

The causal digraph for the short circulation was constructed using the graphical user interface, and the diagnosis was performed for the faulty data which was collected during closed loop operation of the APROS model. The residuals and alarms were generated and the fault origin as well as the fault nature were determined and shown in the MATLAB graphic user interface automatically. Examples of the global residual tests for the mass flow rate through the headbox (*tf*), filler consistency in the deculator (*de_fc*), filler consistency in the headbox (*hb_fc*) and filler consistency in the wire pit (*wp_fc*) are shown in figure 6. The fact that these variables do not cause any alarms excludes them from the group of fault origin candidates.

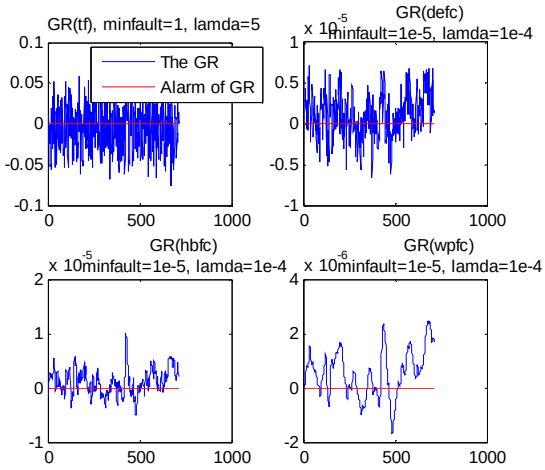

Fig.6. Global tests for *tf*, *de_fc*, *hb_fc* and *wp_fc*

The global tests for the paper quality variables: basis weight (*bw*) and ash rate (*ash*) however fired alarms, even though the quality controllers work well and keep the measurements of these two variables to follow their respective setpoints. The test result for variable *bw* is shown in figure 7, which implies two facts. First of all the, production efficiency has decreased even though the quality of the paper is kept the same. The second fact is that a conflict between control and fault diagnosis exists, since the purpose of the former is to remove unwanted effects of 'disturbances' on the final product quality, which makes fault detection even harder in cases when only a threshold for the variable is utilized.

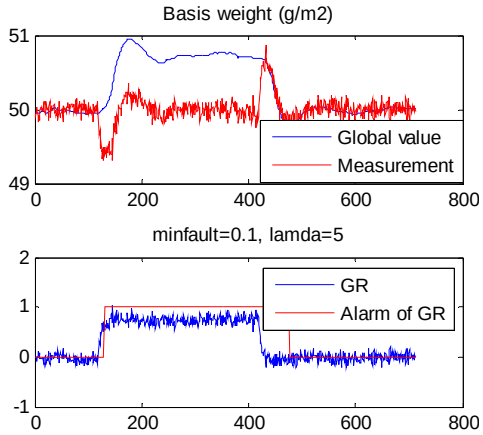

Fig.7. Global test for *bw*

Similar results can be obtained for the variables *de_fic*, *wp_fic* and *hb_fic*, which all have generated alarms for their global tests. So in the causal digraph model in figure 3, there are 5 variables that have alarms for the global tests, which brings forward the demand to find the fault origin in these faulty variables, to find the fault propagation path and to find the nature of the fault. Therefore local residuals were generated and inference based on the rules stated in section 2 was further performed. The local tests for these variables are shown in figure 8 and figure 9 respectively.

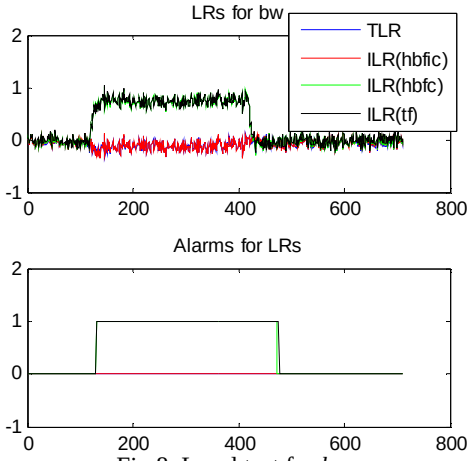

Fig.8. Local test for *bw*

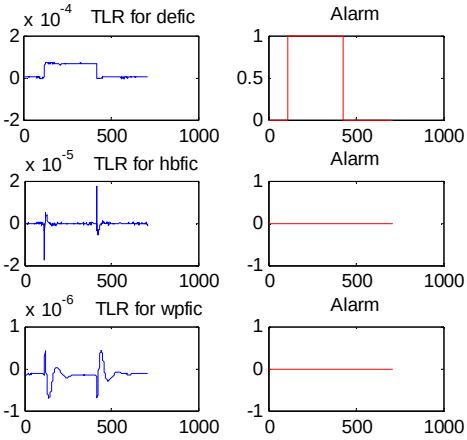

Fig.9. TLR for *de_fic*, *hb_fic* and *wp_fic*

The results in figure 8 imply that the fault is not local and has propagated from the upstream variable *hb_fic*, since the TLR (*bw*) and ILR(*hb_fic*) remove the alarm when the respective measurements from the parent nodes were used. A similar test result was obtained for variable *ash*. According to the same rule, the TLR test for *de_fic* in figure 9 shows that the fault origin is the fiber consistency in the deculator, while other alarmed variables were affected by it.

The fault nature rules further tells that this is a process parameter fault since it propagates through the process globally. The final fault diagnosis is presented by the MATLAB graphical user interface shown in the following figure.

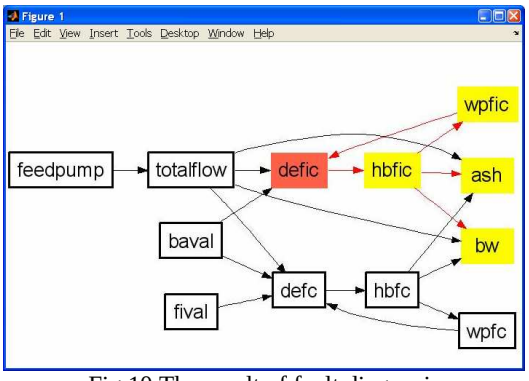

Fig.10.The result of fault diagnosis

6. CONCLUSIONS

In this paper, the ability of the causal digraph method for fault detection and isolation was tested in a simulation environment. The linearity of APROS paper machine model was tested and linear discrete state space models were used to describe the causal relations in the graph. The CUSUM signal-based method was applied to evaluate the generated residuals. The results shown and discussed prove that the causal digraph is a useful fault diagnosis tool.

However like all other methods, causal digraphs also have some drawbacks giving us space to improve the method. First of all, causal digraph only locates the fault on the variable, which will result in some ambiguity in the case of multiple inputs for the variable. In the case study presented in this paper, the fault origin is located as variable *de_fic*, and furthermore the fault is correctly classified as a process fault, while the actual fault existing between one of the parent variables and *de_fic* unfortunately cannot be identified. Another problem is that when a measurement fault is involved in a control loop, the nature of the fault cannot be identified correctly by the fault nature rules. Finally, the rules developed so far for the fault diagnosis only utilize the local pattern produced by the causal diagraph, which means that only the causal relationship between parents and children were used for the consistency test, while the reality is that fault can produce a pattern for the whole digraph, i.e. one fault can produce multiple fault origin variables in the graph.

Besides trying to solve some on the above problems we are going to do research on, how to utilize the qualitative and quantitative information for fault recovery and also fault tolerant control could be interesting topic.

ACKNOWLEDGEMENTS

This work is finically supported by the Finnish Funding Agency for Technology and Innovation.

REFERENCES

APROS (2005). The Advanced Process Simulation Environment, http://apros.vtt.fi/, 21st Dec 2005.

Hinckley, D.V. (1971). Inference about the change-point from cumulative sum tests, *Biometrika*, **58**, pp. 509-523.

Iri, M., K., Aoki, E., O'Shima and H., Matsuyama (1979). An algorithm for diagnosis of system failures in the chemical process, *Computer & Chemical Engineering*, **3 (1-4)**, pp.489-493

Leyval, L., S. Gentil and S., Feray-beaumont (1994). Model-based Causal Reasoning for Process Supervision, *Automatica*, **30**, pp. 1295-1306

Montmain, J. and S., Gentil (2000). Dynamic causal model diagnostic reasoning for online technical process supervision, *Automatica*, **36**, pp. 1137-1152

Nikus, M. and A., Bulsari (1995). A preliminary study on identification and Kalman filtering with recurrent neural networks, Technical Report 95-5, Heat Eng. Lab., Åbo Akademi University, Åbo, 1995

Saxén B. and H., Saxén (1994). NNDT - A neural network development tool - User's guide, Technical Report 94-8, Heat Eng. Lab, Åbo Akademi University, Åbo, 1994

Shih R. and L. Lee (1995). Use of Fuzzy Cause-Effect Digraph for Resolution Fault Diagnosis for Process Plants. 1&2. Fuzzy Cause-Effect Digraph, *Industrial & Engineering Chemistry Research*, **34**, pp. 1688-1717.